Investigation of Orthogonal Experiment for Fabrication of a Soldering Joint for a 4-T HTS Coil

Feng Zhou, Junsheng Cheng, Ying Xu, Shousen Song, Yinming Dai, and Qiuliang Wang, *Senior Member, IEEE*

***Abstract*—The joining process of individual BSCCO conductors is inevitable because the double pancake coils need to be connected with each other. Since the resistance characteristics of the joint can affect the stability of nuclear magnetic resonance system seriously, we did a research on soldering joint in this paper. As resistance characteristics of a soldering joint can vary with conditions such as joint length, thickness, temperature, and so on, we conducted short sample joint experiments with orthogonal experimental design. The significance of each condition's influence was quantitatively calculated, and an appropriate soldering condition was put forward, under which the lowest joint resistance can be obtained. We also applied this appropriate soldering condition to fabricate joints for a 4-T high-temperature superconductivity coil and tested its practical electrical properties.**

***Index Terms*—BSCCO, soldering joint, orthogonal experiment, electrical properties, high-temperature superconductivity (HTS) coil.**

I. Introduction

In recent years, there are many researches conducted on the application of BSCCO in a high-temperature superconductivity (HTS) coil for nuclear magnetic resonance (NMR) system. The joining process of two separate BSCCO tapes is one of the most indispensable techniques of HTS coil for NMR system [1]–[3]. Generally speaking, there are two types of joint techniques: superconducting joint and nonsuperconducting joint. The soldering joint is one of the most common techniques in nonsuperconducting joint [4], [5]. One of the key points is to acquire a low resistance to avoid heating. There have been some researchers conducting BSCCO short sample joint experiments to analyze the factors affecting joint resistance; however, they only did a relatively comprehensive analysis on how each single factor affected joint resistance, without comparing the significance of each factor's influence [6], [7].

Our research uses mathematical means to research the significance of each factor affecting joint resistance; finds an appropriate condition for a soldering joint, under which the lowest joint resistance can be obtained. In this paper, experimental analysis of resistance characteristics for short sample between two BSCCO tapes was conducted. The experiment was conducted in orthogonal experimental method with 5 factors and 2 levels in each (length, thickness, temperature, joint geometry and disposition of stainless steel layer). Moreover, to control these factors precisely in the experiment, we developed a convenient soldering machine capable of soldering on various conditions in this research. The resistance characteristics of each short sample were measured from the V–I curve. We utilized the appropriate condition to fabricate joints for a 4 T HTS coil and tested the coil's electrical characteristics.

Manuscript received May 8, 2014; accepted June 9, 2014. Date of publication June 25, 2014; date of current version July 3, 2014. This work was supported by the National Natural Science Foundation of China under Grant 50925726 and Grant 10755001 and by the National Major Scientific Equipment R&D Project under Grant ZDYZ2010-2.

The authors are with the Institute of Electrical Engineering, Chinese Academy of Science, Beijing 100190, China (e-mail: zhoufeng@mail.iee.ac.cn; qiuliang@mail.iee.ac.cn).

Color versions of one or more of the figures in this paper are available online at http://ieeexplore.ieee.org.

Digital Object Identifier 10.1109/TASC.2014.2331452

II. Short Sample Experiment

A. Soldering Device

A convenient soldering device was developed. To control the factors aforementioned easily, the principles of design were:

(I) Easy to adjust the joint length.
(II) Easy to adjust the joint thickness and pressure is uniformly distributed on the tapes.
(III) Easy to adjust the temperature and heat is uniformly distributed on the tapes.
(IV) Access to both lap joint and bridge joint.

Fig. 1 shows the soldering machine. The soldering machine constitutes two separate parts: soldering part and temperature control part. The soldering part is made of stainless steel, which conducts heat easily and consists of a cover and a supporter. In addition, the groove between the cover and the supporter is coated with vacuum grease to avoid the tape being soldered with the soldering part. Two heating bars and a thermocouple temperature sensor are inserted into the soldering part to adjust and monitor the temperature, respectively. The pressure on tape was applied by the cover's gravity and the pressure applied on the top of the cover. Adding some thin stainless steel shims between the cover and the supporter can adjust the joint thickness easily.

The temperature control part is connected with the heating bars and the thermocouple temperature sensor. We can set the target temperature and observe the real-time temperature. According to the real-time temperature and the target temperature, it can control the current of the heating bars to make the soldering part reach a stable target temperature (with a PID method, the max error is $\pm 2^{\circ}$C).

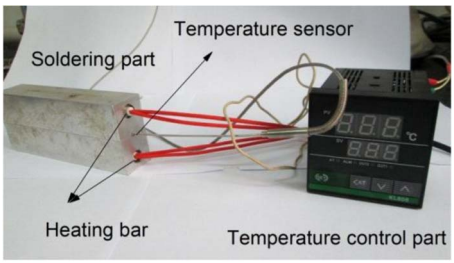

(a)

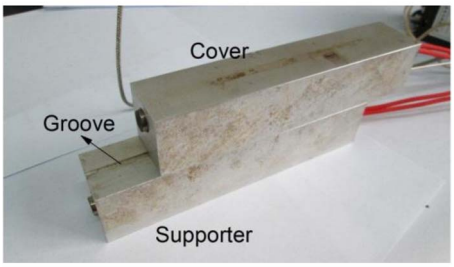

(b)

Fig. 1. Pictures of the soldering machine, (a) the whole part and (b) the soldering part.

TABLE I
CHARACTERISTICS OF BSCCO TAPE

Average thickness	0.23-0.25 mm
Minimum width	4.7 mm
Maximum width	5.0 mm
Max. Rated tensile stress	280 MPa[i,ii]
Max. Rated tensile strain	0.3%[i,ii]
Max. Rated compressive strain	0.15%[i,ii]
Ic	145 A[ii]

[i] Greater than 95% Ic retention
[ii] 77K, self-field, 1 μ V/cm

B. Joint Process

The BSCCO tapes are supplied by American Superconductor (AMSC). They are fabricated in powder-in tube (PIT) method with multifilamentary high-temperature superconductor wire encased in a silver matrix and laminated with stainless steel to provide high mechanical strength. The main characteristics of the tapes are shown in Table I.

In the experiment, all the BSCCO tapes are cut in 150 mm in length; PbSnBi (Pb, 20%–25%; Bi, 37%–43%; Sn, the rest; made by heating and melting method) is used as the solder material with melting point around 110 °C; the cooling time from soldering temperature to room temperature is 10 min. The samples are under constant pressure during the soldering and cooling process. The stainless steel lamination of some samples is manually removed by heat treatment. Two joint geometries are employed, i.e., lap joint and bridge joint, whose schemes are shown in Fig. 2.

C. Results and Discussions

The orthogonal experimental table $L_8(2^7)$ is used with 5 factors and 2 levels in each, which is shown in Table II. For an orthogonal experimental table, there are generally two analyzing methods: range analysis and variance analysis. Range analysis is simple and easy to understand, but it cannot separate the experimental error's influence. So variance analysis is used here to fill the gap. In order to do variance analysis, the orthogonal experimental table must contain blank column to serve as the error term. In our design, there are only 5 factors to analyze, so the column F and G serve as the error column. More details about orthogonal experiment design and analysis can be seen in [8].

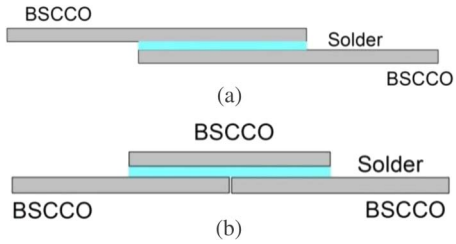

Fig. 2. Two joint geometries, (a) lap joint and (b) bridge joint.

Eight joint samples are fabricated according to each condition; one of the samples is shown in Fig. 3. The resistances of the samples are tested by V–I characteristic curves measurement at 77 K in a saturated liquid nitrogen bath by four-probe method; the results are shown in Table II.

In Table II, $x_{ij}, i = 1, 2, \cdots, m$, m is the level number, here $m = 2$; $j = 1, 2, \cdots, r$, r is the number of repeating level, here $r = 4$; n is the number of experiments, here $n = 8$; the total sum of square of deviations

$$S_T = Q_T - CT, \tag{1}$$

where the quadratic sum

$$Q_T = \sum_{i=1}^{m}\sum_{j=1}^{r}(x_{ij})^2, \tag{2}$$

the correction coefficient

$$CT = \frac{T^2}{n}; \tag{3}$$

the sum

$$T = \sum_{i=1}^{m}\sum_{j=1}^{r}x_{ij}; \tag{4}$$

each factor's sum of square of deviations

$$\begin{cases} S_A = Q_A - CT \\ S_B = Q_B - CT \\ \vdots \end{cases}, \tag{5}$$

where

$$Q_A, Q_B, \cdots = \frac{1}{r}\sum_{i=1}^{m}\left(\sum_{j=1}^{r}x_{ij}\right)^2; \tag{6}$$

the sum of results at level "1"

$$K_{1A}, K_{1B}, \cdots = \sum_{i=1}^{r}x_{1i}; \tag{7}$$

the sum of results at level "2"

$$K_{2A}, K_{2B}, \cdots = \sum_{i=1}^{r}x_{2i}. \tag{8}$$

TABLE II
ORTHOGONAL EXPERIMENTAL TABLE

factor / n	A (joint length)	B (joint thickness)	C (joint geometry)	D (disposition of stainless steel layer)	E (soldering temperature)	e(error) F	e(error) G	Resistance results (x_{ij}*$10^{-7}\Omega$)
1	1(50 mm)	1(0.5 mm)	1(lap joint)	1(remove)	1(180 ℃)	1	1	1
2	1	1	1	2(remain)	2(220 ℃)	2	2	8.2
3	1	2(0.8 mm)	2(bridge joint)	1	1	2	2	7
4	1	2	2	2	2	1	1	20
5	2(130 mm)	1	2	1	2	1	2	0.8
6	2	1	2	2	1	2	1	1.75
7	2	2	1	1	2	2	1	6.5
8	2	2	1	2	1	1	2	10
$\mathbf{K_{1f}}$	36.2	11.75	25.7	15.3	19.75	31.8	29.25	T=55.25 CT=381.57 S_T=281.62
$\mathbf{K_{2f}}$	19.05	43.5	29.55	39.95	35.5	23.45	26	
$\mathbf{Q_f}$	418.34	507.58	383.42	457.52	412.58	390.28	382.89	
$\mathbf{S_f}$	36.76	126.01	1.85	75.95	31.01	8.72	1.32	

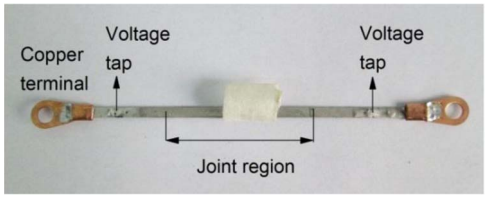

Fig. 3. Soldering joint sample.

TABLE III
VARIANCE ANALYSIS TABLE

Factor	Sum of square of deviations (S)	Freedom degree (f)	Variance (V)	F value	Significance
A	36.76	1	36.76	7.33	Slightly significant
B	126.01	1	126.01	25.11	Very significant
C	1.85	1	1.85	0.37	Not significant
D	75.95	1	75.95	15.14	Significant
E	31.01	1	31.01	6.18	Slightly significant
e	10.04	2	5.02		
T	281.62	7			

In the experiment, the resistance characteristic of the soldering joint is related to 5 factors; each factor has 2 levels; so there will be $2^5 = 32$ experiments in a complete analysis. Using orthogonal experimental method $(L_8(2^7))$, there only need to be eight experiments, which minimizes the number of experiments. Also, with orthogonal experiment, the significance of each factor's influence on joint resistance can be quantitatively calculated, and the optimum soldering condition can be put forward. The variance analysis result is shown in Table III.

In Table III, the total freedom degree

$$f_T = n - 1; \tag{9}$$

the factors' freedom degree

$$\begin{cases} f_A = level\ number\ of\ A - 1 = m - 1 \\ f_B = level\ number\ of\ B - 1 = m - 1 \\ \vdots \end{cases}; \tag{10}$$

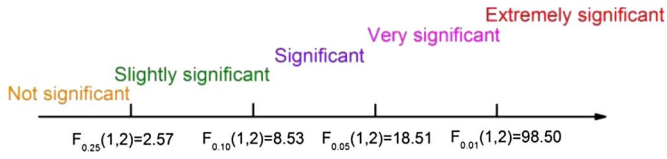

Fig. 4. Decision rule of significance.

the error's freedom degree

$$f_e = f_T - (f_A + f_B + \cdots); \tag{11}$$

variance

$$\begin{cases} V_A = \frac{S_A}{f_A} \\ V_B = \frac{S_B}{f_B} \\ \vdots \\ V_e = \frac{S_e}{f_e} \end{cases}; \tag{12}$$

F value

$$\begin{cases} F_A = \frac{V_A}{V_e} \\ F_B = \frac{V_B}{V_e} \\ \vdots \end{cases}. \tag{13}$$

According to the F value of each factor and the given significanceF_α, we can evaluate whether each factor's influence on resistance is significant or not relative to experimental error's influence on resistance. The greater the F value is, the more significant the factor's influence is. According to $f_A = f_B = \cdots = f_E = 1$, $f_e = 2$ and significance level $\alpha = 0.01$, 0.05, 0.10, 0.25, the critical F value F_α can be referred to the F value distribution table:

$$\begin{cases} F_{0.01}(1,2) = 98.50 \\ F_{0.05}(1,2) = 18.51 \\ F_{0.10}(1,2) = 8.53 \\ F_{0.25}(1,2) = 2.57 \end{cases} \tag{14}$$

so the decision rule of significance is shown in Fig. 4.

From Tables II and III, we can draw some conclusions as follows:

(I) According to F value in Table III, the significance of each factor's influence on joint resistance is $B \rightarrow$ D $\rightarrow$ A $\rightarrow$

TABLE IV
OPTIMUM SOLDERING CONDITION

Joint thickness (mm)	Disposition of stainless steel layer	Joint length (mm)	Soldering temperature (℃)	Joint geometry
0.5	Remove	130	180	Lap joint

TABLE V
SELECTED SPECIFICATIONS OF THE DOUBLE PANCAKE COIL WOUND WITH 200 M TAPE

I.D.(mm)	O.D.(mm)	Height(mm)	Turns	Inductance(H)
140	262	9.5	156+156	0.18

TABLE VI
SELECTED SPECIFICATIONS OF THE WHOLE HTS COIL

I.D.(mm)	O.D.(mm)	Height(mm)	Double pancakes	Inductance(H)
140	262	165	17	3.06

$\mathrm{E} \rightarrow \mathrm{C}$; that is joint thickness > disposition of stainless steel layer > joint length > soldering temperature > joint geometry.

(II) According to K_{1f} and K_{2f} in Table II, to reach the lowest joint resistance, the optimum soldering condition is $\mathrm{B_1D_1A_2E_1C_1}$, which is shown in Table IV.

III. HTS COIL EXPERIMENT

Note that it is generally agreed, because of self-field, the electrical characteristics of joint in practical use is much worse than the short sample [9], [10]. To verify the joints' electrical characteristics in practical use, we utilized the optimum soldering condition to fabricate joints for a 4 T HTS coil.

A. Joint Fabrication

The 4 T HTS coil was made of 17 BSCCO double pancake coils. Each double pancake coil was wound with 200 m long of the same BSCCO tape as shown in Table I. Selected specifications of the double pancake coil and the whole HTS coil are shown in Tables V and VI.

In order to connect the 17 double pancakes (1∼17) in series, there needs to be 16 joints between them. Each of the joint was fabricated according to the optimum soldering condition. We still chose PbSnBi as the solder material because of its stability and controlled the soldering conditions precisely with a self-made curve soldering machine. The whole HTS coil is shown in Fig. 5.

B. Measurement and Results

We still used the four-probe method to test the electrical characteristics of each double pancake at 77 K in a saturated liquid nitrogen bath. Considering that the self-field of the whole HTS coil was symmetry, we only tested 1∼8 on the top. The test of every double pancake comprised of the double pancake itself and the joint, which is connected to the next. The testing result is shown in Fig. 6 and Table VII. Unfortunately, the maximum

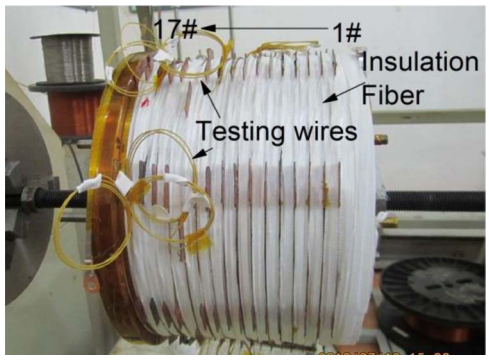

Fig. 5. Whole HTS coil (wound with insulation fiber).

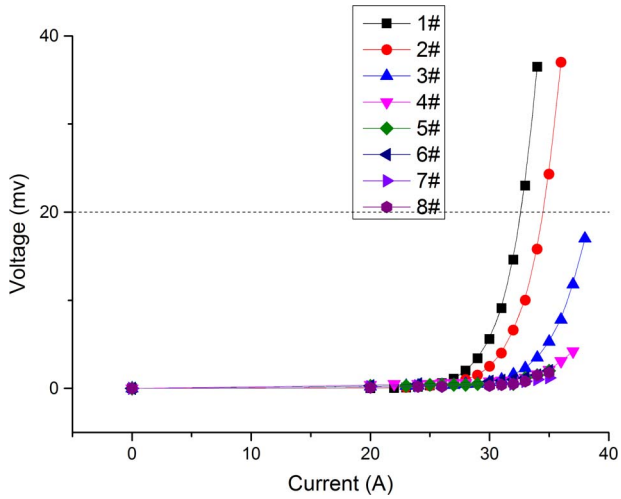

Fig. 6. V–I curve of 1∼8 double pancakes.

TABLE VII
WHOLE RESISTANCES OF 1∼8 DOUBLE PANCAKES

	Resistance (Ω)		Resistance (Ω)
1#	$3.41*10^{-6}$	5#	$2.27*10^{-6}$
2#	$5.43*10^{-6}$	6#	$3.05*10^{-6}$
3#	$3.23*10^{-6}$	7#	$4.15*10^{-6}$
4#	$5.12*10^{-6}$	8#	$3.26*10^{-6}$

current of power supply in this study was 40 A. In this reason, only the critical current of 1, 2, and 3 could be measured.

We assume that the double pancakes do not have resistance in nonquench state; thus, the whole resistance got from test can be interpreted as the joint resistance.

From Table VII, it can be seen that the resistances of joints in practical use are larger than that of short samples; this is because the joint in practical use has a bending diameter, which enlarges resistance; the joint resistance has no certain relationship with location, but owing to the perpendicular component of the self-field, the critical current (according to the 1 μV/cm criteria) has a clear relationship with location: the double pancakes on the ends have a smaller critical current.

Since the double pancakes are connected in series, the critical current of the whole HTS coil is determined by the double pancakes' least critical current, which is ∼32 A (critical current of 1), at 77 K (shown in Fig. 6). We use ANSYS to establish a $(1/2)$ axisymmetric model of this coil to calculate its magnetic field distribution. The result shows that, at 32 A, the center

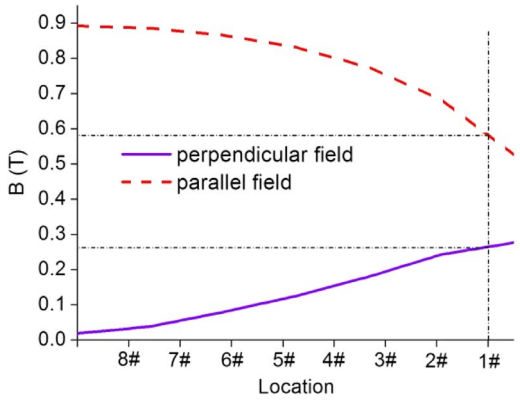

Fig. 7. Perpendicular and parallel field on 1∼8 double pancakes (at 32 A).

TABLE VIII
PERPENDICULAR AND PARALLEL FIELD ON 1, 2, 3 AT THEIR CORRESPONDING CRITICAL CURRENT

Double pancake	Critical current (A)	Perpendicular field (T)	Parallel field (T)
1#	~32 A	0.264	0.582
2#	~34 A	0.254	0.731
3#	~38 A	0.231	0.894

field is 0.83 T and the distribution of perpendicular and parallel field on 1∼8 double pancakes is shown in Fig. 7. Similarly, we can also calculate the distribution of perpendicular and parallel fields on 2, 3 double pancakes at their corresponding critical current of 2 (∼34 A) and 3 (∼38 A), respectively. The summary result is shown in Table VIII.

The HTS coil will finally work in a 4.2 K environment. The critical current at 4.2 K is at least 6 times of the one at 77 K, so the HTS coil's critical current at 4.2 K is at least ∼190 A, which is larger than the operation current of ∼154 A (4 T). Therefore, the fabrication of these joints can satisfy our requirement.

IV. CONCLUSION

In this paper, we did a research on a soldering joint between two separate BSCCO tapes. The BSCCO tapes were soldered on various conditions varying with joint length, thickness, temperature, joint geometry, and disposition of stainless steel layer. According to the result from a short sample orthogonal experiment we conducted, we got the significance of each factor's influence on joint resistance is joint thickness $>$ disposition of stainless steel layer $>$ joint length $>$ soldering temperature $>$ joint geometry and developed an optimum condition for a soldering joint, under which the lowest joint resistance can be obtained. We also utilized the optimum soldering condition to fabricate joints for a 4 T HTS coil to verify the joints' electrical characteristics in practical use; each joint of the HTS coil has a resistance of $2 \sim 6 \times 10^{-6}\ \Omega$ and the HTS coil's critical current is ∼32 A at 77 K and ∼190 A at 4.2 K, which is larger than the 4 T operation current of ∼154 A. It has been demonstrated that the fabrication of these joints can satisfy our requirement.

REFERENCES

[1] J. H. Kim, B. K. Ji, J. Joo, C. W. Yang, and W. Nah, "Superconducting joint between Bi-Pb-Sr-Ca-Cu-O superconductor tapes," *IEEE Trans. Appl. Supercond.*, vol. 10, no. 1, pp. 1182–1185, Mar. 2000.

[2] K. Fukushima *et al.*, "Persistent mode operation of $Bi_2Sr_2Ca_1Cu_2Ox/Ag$ stacked double pancake coils with superconducting joints," *Japanese J. Appl. Phys.*, vol. 36, no. 11A, pp. L1433–L1435, 1997.

[3] Q. L. Wang *et al.*, "Design of open high magnetic field MRI superconducting magnet with continuous current and genetic algorithm method," *IEEE Trans. Appl. Supercond.*, vol. 19, no. 3, pp. 2289–2292, Jun. 2009.

[4] Q. L. Wang *et al.*, "Development of high magnetic field superconducting magnet technology and applications in China," *Cryogenics*, vol. 47, no. 7/8, pp. 364–379, Jul./Aug. 2007.

[5] Q. L. Wang, "High field superconducting magnet: Science, technology and applications," *Progr. Phys.*, vol. 33, no. 1, pp. 1–23, 2013.

[6] P. V. Shoaff, Jr., Y. S. Hascicek, J. Schwartz, and S. W. Van Sciver, "An investigation of the characterization and development of HTS joints in BSCCO 2212/Ag composites," *IEEE Trans. Appl. Supercond.*, vol. 7, no. 2, pp. 1695–1698, Jun. 1997.

[7] C. Y. Shigue, C. A. Baldan, and E. Ruppert-Filho, "Evaluation of current transfer in Bi-2223/Ag composite tapes," *Physica C*, vol. 408–410, pp. 698–699, Aug. 2004.

[8] J. Kiefer, "Optimum experimental designs," *J. R. Stat. Soc., Series B (Methodological)*, vol. 21, no. 2, pp. 272–319, 1959.

[9] M. H. Sohn *et al.*, "Joint resistances between two parallel high T_c superconducting tapes," *IEEE Trans. Appl. Supercond.*, vol. 13, no. 2, pp. 1764–1767, Jun. 2003.

[10] Q. L. Wang, *Practical Design of Magnetostatic Structure Using Numerical Simulation*. Hoboken, NJ, USA: Wiley, 2013.